Observation of 5*f* electrons in the itinerant limit: Three-dimensional electronic structure of UB_2

Takuo Ohkochi,[1] Shin-ichi Fujimori,[1] Hiroshi Yamagami,[1,2] Tetsuo Okane,[1] Yuji Saitoh,[1] Atsushi Fujimori,[3] Yoshinori Haga,[4] Etsuji Yamamoto,[4] and Yoshichika Ōnuki[5]

[1]*Synchrotron Radiation Research Unit, Japan Atomic Energy Agency, Sayo, Hyogo 679-5148, Japan*

[2]*Department of Physics, Faculty of Science, Kyoto Sangyo University, Kyoto 603-8555, Japan*

[3]*Department of Physics, University of Tokyo, Hongo, Bunkyo-ku, Tokyo 113-0033, Japan*

[4]*Advanced Science Research Center, Japan Atomic Energy Agency, Tokai, Ibaraki 319-1195, Japan*

[5]*Graduate School of Science, Osaka University, Toyonaka, Osaka 560-0043, Japan*

(Received 12 May 2008; published 13 October 2008)

We have derived the three-dimensional band structure and Fermi surfaces of itinerant uranium compound UB_2 by soft x-ray angle-resolved photoelectron spectroscopy. We have observed clear energy dispersions and Fermi surfaces with large contribution from the U 5*f* states. The obtained results have been compared with the result of band-structure calculation within the local-density-functional approximation as well as the results of de Haas–van Alphen (dHvA) study. The qualitative agreement has been obtained in the size and topology of the Fermi surfaces with the band-structure calculation and the dHvA measurement. Meanwhile, their band structure near the Fermi level is slightly different from the calculation. This might be due to a dynamic renormalization beyond the local-density approximation band calculations even in the very itinerant 5*f* compound.

DOI: 10.1103/PhysRevB.78.165110 PACS number(s): 71.18.+y, 71.20.−b, 71.27.+a, 79.60.−i

I. INTRODUCTION

In recent years, a different class of unconventional superconductors has been discovered in transuranium compounds and attracted much attention.[1] These superconductors share a unique position due to their relatively high superconducting transition temperatures T_c [18 K for $PuCoGa_5$,[2] 8.7 K for $PuRhGa_5$,[3] and 5 K for $NpPd_5Al_2$ (Ref. 4)] compared with uranium heavy-fermion superconductors. These remarkable discoveries recall the long-standing question of *f*-electron physics: How are actinide 5*f* electrons involved in their band structures and Fermi surfaces (FSs), and how can they be described theoretically? To address this question, it is essential to clarify, first of all, the validity of the theoretical description of the 5*f* electronic states within a local-density approximation (LDA) when the 5*f* electrons are in the itinerant limit. Angle-resolved photoemission spectroscopy (ARPES) has been applied for various actinide compounds since the detection of the 5*f* band dispersion is the most direct test of various theoretical models for the 5*f* states.[5–7] Nevertheless, the detection of energy dispersion in actinide 5*f* states has not been successful due to the drawbacks in the conventional ARPES experiments such as the high surface sensitivity or the low photoionization cross section of the actinide 5*f* states in comparison with ligand *s*, *p*, and *d* states.

In this study, we have performed $h\nu$-dependent ARPES in the soft x-ray region (SX-ARPES) on a very itinerant 5*f* compound UB_2. We have observed unambiguous 5*f*-selective band dispersions and found that they form FSs of this compound. It is demonstrated that they are basically described by a band-structure calculation based on LDA with renormalization due to a static electron correlation. SX-ARPES is a recently developed technique which can be utilized to observe bulk electronic structures of materials.[8,9] This is a particularly powerful experimental technique for uranium compounds due to its high sensitivity to the 5*f* states.[10,11] While we have measured the SX-ARPES spectra of the itinerant 5*f* compound $UFeGa_5$ in previous work[10] and found that the gross features of the band structure and FSs can be well described by the band-structure calculation, only a limited part of the Brillouin zone was explored, and a detailed comparison between the experiment and the band-structure calculation could not be made.

UB_2 is a paramagnetic compound with the hexagonal AlB_2-type structure in which a two-dimensional uranium- and boron-atoms network are stacked alternately along the (0001) direction. The interatomic U-U spacing in the two-dimensional plane is 3.123 Å, which makes a large direct *f*-*f* overlap. Its electronic specific-heat coefficient γ_e is as low as 10.3 $mJ/(K^2\,mol)$ which is comparable to the value obtained by the LDA band-structure calculation [7.29 $mJ/(K^2\,mol)$].[12] The de Haas–van Alphen (dHvA) measurement was performed for this compound, and the observed branches were well explained also by the LDA band-structure calculation.[13] Therefore, UB_2 is considered to have itinerant 5*f* electronic states, and it gives a unique opportunity to observe directly the itinerant 5*f* electronic states.

II. EXPERIMENTAL

The ARPES experiments were carried out at the SPring-8 BL23SU. The energy resolution was 120–130 meV in the ARPES experiments with $h\nu$=450–500 eV. The angular resolution was ±0.15°, and the corresponding momentum resolution for the $k_{\parallel}$ direction was about 0.06 $Å^{-1}$. Since the size of the Brillouin zone of UB_2 for the Γ-*K* direction is ~1.34 $Å^{-1}$, about 20 individual *k* points along this direction can be resolved in the present experiments. The momentum broadening for the $k_{\perp}$ direction due to the finite escape depth of photoelectrons (10–15 Å) is estimated to be 0.06–0.1 $Å^{-1}$. This is much smaller than the size of the Brillouin zone for the *c* axis (1.58 $Å^{-1}$), but substantial contributions from surrounding band structures are not negligible when the bands have strong dispersions along the $k_{\perp}$ direction.[15] The position of the ARPES scan in the Brillouin zone was estimated by assuming a free-electron final-state

model in which the momentum of incident photons has been taken into account. The detail of the calculation is described in Ref. 10. The value of the inner potential was determined to be $V_0=12$ eV by measuring the photon energy dependence of ARPES spectra in the energy range of $h\nu=440-550$ eV. Although $k_\perp$ changes as a function of the detection angle of photoelectrons, this is negligible for the present experimental setup. Accordingly, the ARPES spectra shown in the present study reflect the contributions from a specific high-symmetry line with a finite broadening for the $k_\perp$ direction. The sample temperature was 20 K during the course of measurement. The position of the Fermi level (E_F) was determined by referring to the E_F of evaporated gold films. A high-quality UB_2 single-crystal ingot was grown by the Czochralski method. The sample was cleaved *in situ* along the (0001) plane prior to the experiment. The energy-band structure and FS of UB_2 were calculated by using the relativistic linearized augmented plane-wave (RLAPW) method. All electrons including core states are solved by the Dirac one-electron equation with an exchange and correlation potential in LDA.[14] The detail of the calculation is described in Ref. 13.

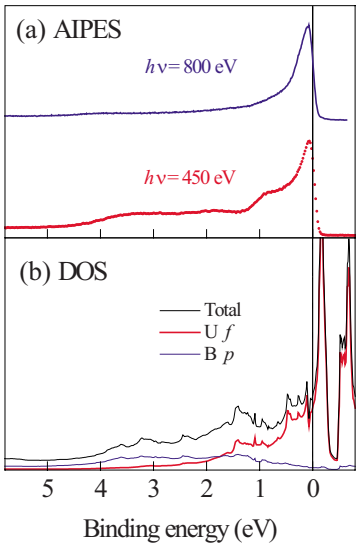

FIG. 1. (Color online) (a) Angle-integrated photoemission spectra (AIPES) measured at $h\nu=450$ and 800 eV. (b) Calculated U f and B p partial DOS and total DOS.

III. RESULTS AND DISCUSSION

Figure 1(a) shows the angle-integrated photoemission spectra (AIPES) of UB_2 measured at $h\nu=450$ and 800 eV. The spectra have a sharp peak just below E_F and show a long tail toward the higher binding-energy sides. In the spectra measured at $h\nu=450$ eV, the broad and weak features were observed in the energy range of $E_B=1.5-4$ eV. According to the atomic photoionization cross-section calculation,[16] the contributions from the U $5f$ states are dominant in these photon energies, and the ones from the other states are smaller by 1–2 orders of magnitude. Meanwhile, the relative photoionization cross section of the U $5f$ states to the B $2s,p$ states increases by the factor of about three as the photon energy increases from 450 to 800 eV. This suggests that, although the contributions from the U $5f$ states are dominant in these spectra, some weak contributions from B p states should be observed in the spectra measured at $h\nu=450$ eV. Therefore, the sharp peak structure just below E_F is ascribed to the contributions mainly from the U $5f$ states, while the broad feature extended around $E_B=1.5-4$ eV is ascribed to the contributions mainly from the B $2s,p$ states. Here, it should be noted that the U $5f$ states have relatively simple and sharp asymmetric line shapes, and the additional satellite structure, which has been observed in the strongly correlated uranium compounds, was not recognized.

Figure 2(a) shows an image plot of the ARPES spectra of UB_2 measured along several high-symmetry lines. The hexagonal Brillouin zone of UB_2 is also shown. The ARPES

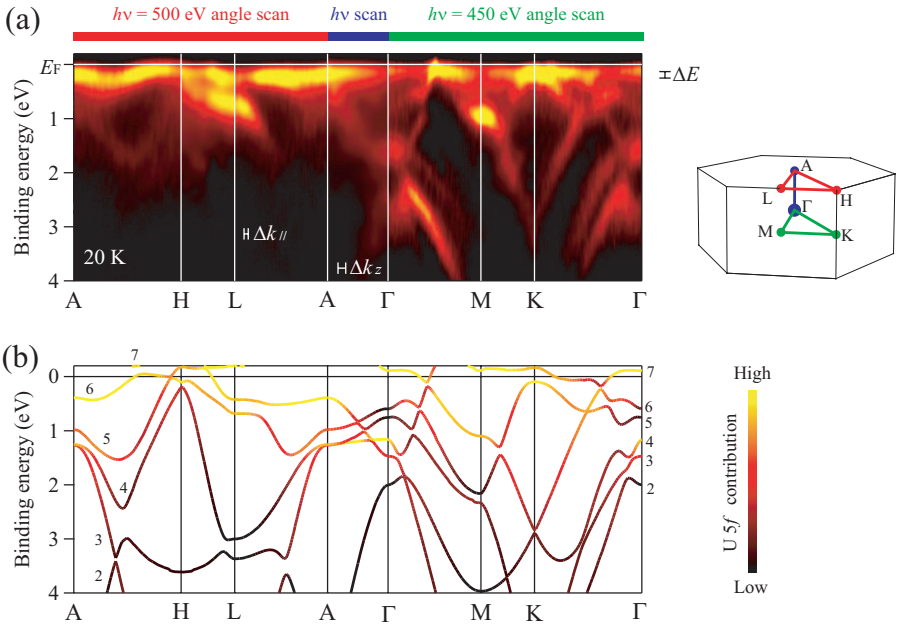

FIG. 2. (Color) (a) ARPES spectra image of UB_2 measured along several high-symmetry lines. The Brillouin zone is also shown. (b) The corresponding calculated energy-band structure of UB_2. The degrees of the contribution from U $5f$ states are indicated by their colors.

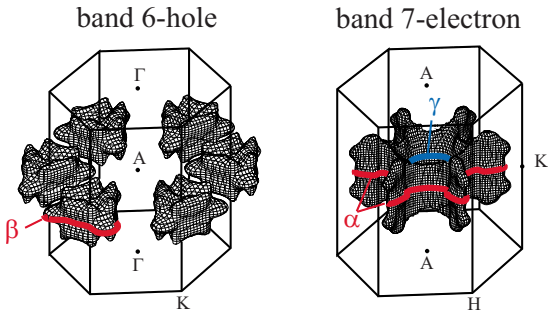

FIG. 3. (Color online) Calculated Fermi surfaces around the *A*-*L*-*H* and Γ-*M*-*K* planes. The branches observed by dHvA experiment are indicated as α, β, and γ.

spectra in the *A*-*H*-*L* plane and those in the Γ-*M*-*K* plane were obtained by changing the detection angle of photoelectrons with $h\nu$=500 and 450 eV, respectively. Meanwhile, the spectra along the *A*-Γ direction were measured by changing the photon energies with a fixed photoelectron detection angle. Each spectrum has been normalized to the area of the energy distribution curve (EDC). Some very complex dispersive features were clearly observed. In the energy range from E_F to 1 eV, the relatively flat energy dispersions with sharp peak structure were recognized. Some bands show dramatic intensity variation just below E_F as a function of momenta, suggesting they cross E_F. Since they have strong intensities in this photon energy range, they are attributed to the contributions mainly from the U 5*f* states. In the high binding-energy region, rapidly dispersing bands were also clearly observed. These spectra show much clearer dispersions than those observed in the previous study,[10] and therefore the U 5*f* states have very itinerant character.

Figure 2(b) shows the theoretical band dispersions obtained by the LDA calculation. The degree of contribution from the U 5*f* states, defined as the strength of the *f* orbital in the wave function of valence electrons at the uranium site, is indicated by a color scale. It is shown that the gross features of experiential ARPES spectra are well explained by the calculation. The agreement is recognized not only in the shape of the bands, but also in the degree of the 5*f* contribution. For example, the near E_F part of experimental ARPES spectra can be explained by the calculated bands 5–7. In addition, the rapidly dispersing bands observed in the deep binding-energy region (1.5–4 eV) are also well reproduced by the bands 2–4, which are expected to have substantially small but nonzero contribution from the U 5*f* states. The U 5*f* electrons are well hybridized with the B 2*s*,*p* states and form very itinerant quasiparticle states.

We further discuss the FS as well as the band structure near E_F. Before we discuss the experimental FSs, we show the calculated FSs and their relationship with the result of the dHvA measurement.[13] Figure 3 shows the calculated FSs. In the band-structure calculation, the pancakelike hole FS centered at the *H* point and the crownlike electron FS centered at the Γ point were obtained. In the dHvA measurement, three main branches were observed and have been attributed to those found in the calculated FSs. "α," "β," and "γ" represent the corresponding branches observed by the dHvA experiment. The experimentally determined size of each branch was well explained by the band-structure calculation.

Figure 4(a) shows the experimental FSs in the *A*-*H*-*L* plane, which is obtained by mapping the integrated ARPES intensity within $E_F \pm 25$ meV as a function of k_x and k_y. In this image, the higher-intensity part corresponds to the position of the FS. The triangle-shaped FSs are observed around the *H* points. The calculated FSs are also shown by solid lines. It is shown that this experimental triangle FS is well reproduced by the calculation. Meanwhile, the experimental FS map shows also intense structures along the *H*-*A* direction inside this triangle. To understand the origin of this structure, we have plotted the calculated FSs with $k_\perp \pm 0.05$ Å^{-1} also as dotted lines. Due to the broadening of the ARPES spectra for the $k_\perp$ direction (0.06–0.1 Å^{-1}), which comes from a finite escape depth of photoelectrons, the FS image contains contributions from the slightly shifted $k_\perp$ plane.[15] It is clearly shown that this additional inner structure corresponds well to this slightly shifted FS. Therefore, we attribute this structure to the finite momentum resolution for the $k_\perp$ direction. Figures 4(b) and 4(c) show the band structures along the *A*-*H* and *H*-*L* lines together with the calculated bands. In this figure, we have normalized the spectra with the integrated intensity of the MDC spectra to eliminate the strong contributions from the Fermi cutoff. Then, we made a second derivative along the energy axis to show the peak position more clearly. This procedure makes it possible to observe fine structures around E_F. The behavior of the bands near E_F is well shown in these figures. It is

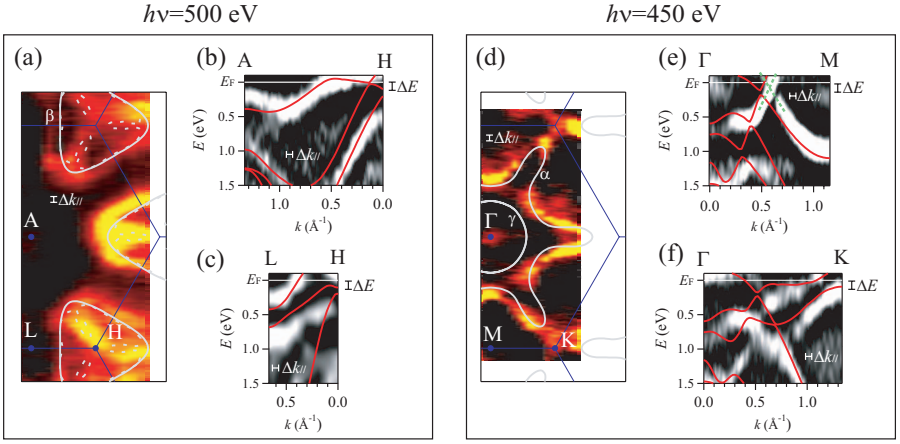

FIG. 4. (Color) Experimental Fermi surfaces and the band structures around E_F. (a) Experimental Fermi-surface image in *A*-*H*-*L* plane. Band structures around E_F in (b) *A*-*L*-*H* direction and (c) *L*-*H* are also shown. The results of LDA calculation are indicated by solid lines. (d)–(f) The same plot as (a)–(c) in the Γ-*M*-*K* plane. The white dotted lines in (a) are the calculated Fermi surfaces with $k_\perp \pm 0.05$ Å^{-1} and the green dotted lines in (e) are a guide for the eyes.

shown that the experimental band forms a large hole pocket around the H point. The feature of this hole FS is well explained by the calculated band 6 and its size is almost identical to the experiment. For the L-H direction, the experimental band near E_F shows a good correspondence to the calculated band 6.

Figure 4(d) shows the same plot as Fig. 4(a) in the Γ-M-K plane. The experimental FS shows a crownlike shape which is ascribable to the branch α. On the other hand, the round shaped FS corresponding to the branch γ is not clearly recognized in this plot. In the ARPES spectra for the Γ-M direction [Fig. 4(e)], two bands approach toward E_F and they cross just below E_F. This suggests the existence of a small electron pocket, as indicated by green dotted lines. This electron pocket surrounded by the α and γ branches is also recognized in the band image along the Γ-K direction [Fig. 4(f)]. Therefore, we conclude that there exists the γ branch (inner circle) in the ARPES spectra, although its size is considerably larger than the calculation.

Here, we note that the width of the experimental FSs in the A-L-H plane [Fig. 4(a)] is considerably large, whereas that in the Γ-M-K plane in Fig. 4(d) is relatively sharp and their widths are comparable to the momentum resolution $\Delta k_{\parallel}$. The fact indicates the additional broadening mostly comes from the finite resolution for the $k_{\perp}$ direction rather than from the energy resolution. As shown in the Fig. 3, since the FSs in the A-L-H plane have a three-dimensional character, the image is broader than that in the Γ-M-K plane which has a two-dimensional character.

To further understand the present experimental data, we have performed a quantitative analysis on the size of the FSs and compared them with the results of the dHvA measurement as well as the LDA calculation. In this analysis, we have estimated the Fermi momentum k_F on the high-symmetry lines. The values are summarized in Table I together with the size of each branch (dHvA frequency F) obtained by dHvA and the LDA calculation.[13] The k_F values for the α and β branches have a fairly good agreement between the ARPES experiment and the calculation, whereas the experimental γ branch is somewhat larger than the calculation. These tendencies are consistent with the values of F obtained by the dHvA measurement. Therefore, we have obtained qualitative agreement between the ARPES and the dHvA experiments. The present study demonstrates that the SX-ARPES can provide direct and qualitative information of the electronic structures of f-electron compounds. Although the topology of the experimental FSs is well explained by LDA calculation as has been concluded from the dHvA study, it seems that the $5f$ band dispersions are slightly different from the LDA calculation in UB_2. Nevertheless, these differences are found only in the energy position of the bands, and essential structures are very similar between the experiment and the calculation, suggesting that the well-renormalized bands form through a strong hybridization. We conclude that the electronic structure of UB_2 can be basically understood by the LDA calculation with a static electron correlation effect. Such information cannot be obtained by magneto-oscillation techniques, demonstrating the importance of SX-ARPES experiments for the study of heavy-fermion compounds.

TABLE I. Distance of α, γ, and β FSs from each center (Fermi momentum k_F) estimated on some high-symmetry lines by ARPES spectra and LDA calculation. Values of dHvA frequency F quoted from Ref. 13 are also shown.

		k_F (Å^{-1})		F ($\times 10^7$ Oe)	
Branch		ARPES	LDA	dHvA[a]	LDA
α	$\Gamma \rightarrow M$	0.59 ± 0.02	0.52	20.5	20.47
	$\Gamma \rightarrow K$	1.08 ± 0.02	1.09		
β	$H \rightarrow A$	0.54 ± 0.05	0.57	9.49	8.31
	$H \rightarrow L$	0.40 ± 0.02	0.38		
γ	$\Gamma \rightarrow M$	0.55 ± 0.02	0.39	6.58	4.82
	$\Gamma \rightarrow K$	0.58 ± 0.03	0.39		

[a]Reference 13.

IV. CONCLUSION

In conclusion, we have performed an $h\nu$-dependent SX-ARPES experiment on the itinerant uranium compound UB_2 and succeeded in obtaining the very clear band dispersions and FSs with large contributions from the $5f$ states, suggesting that the $5f$ electrons in UB_2 have a very itinerant character. Although the entire band structure and the topology of the FSs show good agreement with the LDA calculation, the bands near E_F and the size of the FSs show slight deviation from the calculation. This might be understood by a dynamic renormalization beyond the LDA band calculations, suggesting the validity of the LDA as a good starting point for the description of its band structure as well. At the same time, these results suggest the importance of studying their band structure near E_F as well as their FSs to reveal the nature of electron correlation in the $5f$ states. This information is essential to understand the origin of various properties of uranium compounds such as itinerant magnetism, heavy-fermion superconductivity, and so on.

ACKNOWLEDGMENTS

We thank T. Ito for fruitful discussion. The present work was performed under Proposal No. 2006B3808 at SPring-8 BL23SU and financially supported by a Grant-in-Aid for Scientific Research from the Ministry of Education, Culture, Sports, Science, and Technology Japan under Contract No. 15740226 and REIMEI Research Resources from the Japan Atomic Energy Agency.

[1] J. L. Sarrao and J. D. Thompson, J. Phys. Soc. Jpn. **76**, 051013 (2007).
[2] J. L. Sarrao, L. A. Morales, J. D. Thompson, B. L. Scott, G. R. Stewart, F. Wastin, J. Rebizant, P. Boulet, E. Colineau, and G. H. Lander, Nature (London) **420**, 297 (2002).
[3] F. Wastin, P. Boulet, J. Rebizant, E. Colineau, and G. H. Lander, J. Phys.: Condens. Matter **15**, S2279 (2003).
[4] D. Aoki, Y. Haga, T. D. Matsuda, N. Tateiwa, S. Ikeda, Y. Homma, H. Sakai, Y. Shiokawa, E. Yamamoto, A. Nakamura, R. Settai, and Y. Ōnuki, J. Phys. Soc. Jpn. **76**, 063701 (2007).
[5] A. J. Arko, J. J. Joyce, A. B. Andrews, J. D. Thompson, J. L. Smith, E. Moshopoulou, Z. Fisk, A. A. Menovsky, P. C. Canfield, and C. G. Olson, Physica B **230-232**, 16 (1997).
[6] J. W. Allen, J. Phys. Soc. Jpn. **74**, 34 (2005).
[7] H. Kumigashira, T. Ito, A. Ashihara, H. D. Kim, H. Aoki, T. Suzuki, H. Yamagami, T. Takahashi, and A. Ochiai, Phys. Rev. B **61**, 15707 (2000).
[8] A. Sekiyama, S. Kasai, M. Tsunekawa, Y. Ishida, M. Sing, A. Irizawa, A. Yamasaki, S. Imada, T. Muro, Y. Saitoh, Y. Ōnuki, T. Kimura, Y. Tokura, and S. Suga, Phys. Rev. B **70**, 060506(R) (2004).
[9] T. Claesson, M. Mansson, C. Dallera, F. Venturini, C. De Nadai, N. B. Brookes, and O. Tjernberg, Phys. Rev. Lett. **93**, 136402 (2004).
[10] S. I. Fujimori, K. Terai, Y. Takeda, T. Okane, Y. Saitoh, Y. Muramatsu, A. Fujimori, H. Yamagami, Y. Tokiwa, S. Ikeda, T. Matsuda, Y. Haga, E. Yamamoto, and Y. Ōnuki, Phys. Rev. B **73**, 125109 (2006).
[11] S.-I. Fujimori, Y. Saitoh, T. Okane, A. Fujimori, H. Yamagami, Y. Haga, E. Yamamoto, and Y. Ōnuki, Nat. Phys. **3**, 618 (2007).
[12] E. Yamamoto, T. Honma, Y. Haga, Y. Inada, D. Aoki, N. Suzuki, R. Settai, H. Sugawara, H. Sato, and Y. Ōnuki, J. Phys. Soc. Jpn. **68**, 972 (1999).
[13] E. Yamamoto, Y. Haga, T. Honma, Y. Inada, D. Aoki, M. Hedo, Y. Yoshida, H. Yamagami, and Y. Ōnuki, J. Phys. Soc. Jpn. **67**, 3171 (1998).
[14] H. Yamagami, J. Phys. Soc. Jpn. **67**, 3176 (1998).
[15] V. N. Strocov, J. Electron Spectrosc. Relat. Phenom. **130**, 65 (2003).
[16] J. J. Yeh and I. Lindau, At. Data Nucl. Data Tables **32**, 1 (1985).